

# Studies of non-magnetic impurities in the spin-1/2 Kagome Antiferromagnet

Karol Gregor and Olexei I. Motrunich

*Department of Physics, California Institute of Technology, Pasadena, CA 91125*

(Dated: October 29, 2018)

Motivated by recent experiments on  $\text{ZnCu}_3(\text{OH})_6\text{Cl}_2$ , we study the inhomogeneous Knight shifts (local susceptibilities) of spin 1/2 Kagome antiferromagnet in the presence of nonmagnetic impurities. Using high temperature series expansion, we calculate the local susceptibility and its histogram down to about  $T = 0.4J$ . At low temperatures, we explore a Dirac spin liquid proposal and calculate the local susceptibility in the mean field and beyond mean field using Gutzwiller projection, finding the overall picture to be consistent with the NMR experiments.

## I. INTRODUCTION

Spin liquids are some of the most interesting spin phases that we know to exist theoretically. However experimentally they are hard to achieve because of the competition with magnetically ordered or spin-Peierls phases. Frustration can suppress the order, and one of the promising systems where strong frustration occurs with natural interactions is the nearest neighbor spin 1/2 antiferromagnet on Kagome lattice.

Herbertsmithite  $\text{ZnCu}_3(\text{OH})_6\text{Cl}_2$  contains Kagome layers of spin-1/2 magnetic  $\text{Cu}^{2+}$  moments and has emerged as one such candidate in the recent years.<sup>1,2,3,4,5,6,7,8</sup> Despite the large Curie-Weiss temperature of roughly 300K, experiments observe no magnetic order down to 50mK and no sign of spin freezing or spin-Peierls transition. Various measurements also suggest that there is no gap to excitations, but the nature of the phase remains elusive.

From the beginning,<sup>1,2</sup> it has been appreciated that there is significant amount of disorder in the  $\text{ZnCu}_3(\text{OH})_6\text{Cl}_2$ . Even though impurities do not seem to produce a glassy behavior, they can mask the intrinsic thermodynamic properties of the system such as the spin susceptibility and specific heat. The type of disorder has been clarified to some degree in recent experiments,<sup>5,6,7</sup> which suggest that 5 to 10% of the Cu that would ideally be in the Kagome layers interchange their position with the nonmagnetic Zn between the layers. The picture that is suggested is that the misplaced Cu behave as weakly coupled spins giving rise to the Curie tail and anomalous low-temperature specific heat in the absence of the field, while the misplaced Zn effectively create spin vacancies in the Kagome layers.

There have been many theoretical studies of the clean spin-1/2 Kagome system.<sup>9,10,11,12,13,14,15,16,17,18,19,20,21,22,23,24,25,26,27,28,29</sup> Exact diagonalization studies<sup>9,10,11,12,13,14</sup> indicate no magnetic or spin-Peierls order. Spin wave and series expansion studies<sup>9,15</sup> near several ordered states also indicate that the magnetic orders are not stable (but a recent work<sup>29</sup> suggests that a valence bond solid may be stable). High temperature expansion studies<sup>16,17</sup> for susceptibility of the Heisenberg model provide good quantitative comparison with the experiments and

recent works<sup>18,19</sup> account for possible Curie impurity spin contribution or possible Dzyaloshinsky-Moriya interactions to better match the measurements in the Herbertsmithite.

There are a number of theoretical proposals for spin liquids in the spin-1/2 Kagome.<sup>20,21,22,23,24,25,26,27,28</sup> Of interest to the present work are gapless spin liquids. One is the Algebraic (Dirac) Spin Liquid (ASL) of Hastings<sup>24</sup> and Ran *et al.*<sup>25</sup> whose trial energy is very close to the ground state energy obtained from the exact diagonalization.<sup>25</sup> Recently, Ma and Marston<sup>27</sup> suggested that a different spin liquid with a spinon Fermi surface may be stabilized in the presence of ferromagnetic second-neighbor interactions. Coming from a very different perspective, Ryu *et al.*<sup>28</sup> suggested an Algebraic (Dirac) Vortex Liquid, which bears some resemblance to the ASL in its gapless nature but is a distinct phase.

Impurities modify the properties of the ground state, but at the same time they can be used as a probe of the system, which is our pursuit here. In the NMR context, impurities allow the external magnetic field, which would be strictly  $q = 0$  probe in a clean system, to couple to other potentially more important wavevectors. Despite a large body of work on defects in correlated systems (see Refs. 30,31 and references therein), there have been only few studies of impurities in frustrated magnets.<sup>31,32,33,34</sup> Exact diagonalization study by Dommange *et al.*<sup>33</sup> provides important hints on the behavior of spins near a vacancy in the Kagome antiferromagnet.

Our work is motivated by the recent <sup>17</sup>O NMR measurements of Olariu *et al.*<sup>7</sup>, which shows direct access to the local spin susceptibility. Each oxygen atom feels the magnetic moments of two copper atoms it is connected to, see pictures in Refs. 3,7. Because of the nonmagnetic impurities, some oxygens feel two and some only one spin. The two peaks that are observed in the NMR spectra at high temperatures are explained as coming from these two types of oxygens, neglecting variations in local susceptibility. As the temperature is lowered the peaks first move towards larger susceptibilities and then back to the smaller ones broadening at the same time. At the lowest temperatures only one peak is visible which saturates at small but positive susceptibility value. A strong inhomogeneous broadening was also observed in <sup>35</sup>Cl NMR at low temperatures,<sup>3</sup> but with no clear features that would allow spatial resolution.

In this paper we calculate local susceptibility of Kagome lattice in the presence of nonmagnetic impurities, which are treated as missing spins, by two different methods.

In the first part we use 12-th order high temperature series expansion for the nearest neighbor antiferromagnetic Heisenberg model. We calculate local susceptibility near a single impurity Fig. 1 and for a lattice with 5% of impurities Figs. 2, 3. We obtain quantitatively accurate results down to about  $T \approx 0.4J$ . These can be directly used to test whether the Heisenberg model with spin vacancies applies to the  $\text{ZnCu}_3(\text{OH})_6\text{Cl}_2$ . For this range of temperatures, the local susceptibility goes to the bulk value already at a few lattice spacings from an impurity. On the other hand, the local susceptibility  $\chi_1$  of the spin next to the impurity is larger than the bulk  $\chi_{\text{bulk}}$  by as much as 15-20%. This can be understood by realizing that the Cu near the impurity has only three neighbors instead of four, which directly affects the local Curies-Weiss temperature giving 14% change in  $\chi$  at this temperature. The series expansion study develops this observation systematically to significantly lower temperatures and for all sites. On the other hand, we find that  $\chi_1$  starts to decrease around  $T \approx 0.6J$  and drops below the bulk susceptibility at  $T \approx 0.4J$ , well before the bulk susceptibility starts to decrease at about  $J/6$ .<sup>16,19</sup> This is consistent with the ground state picture found in the exact diagonalization study,<sup>33</sup> where a pair of spins that are both next to impurity forms an almost perfect singlet, so these spins become effectively non-responsive.

One lesson we learn is that even at elevated temperatures one cannot assume the same susceptibility on all Kagome sites. When connecting with the experiments, we suggest to consider at least two different susceptibilities:  $\chi_1$  for the immediate neighbors of impurities and  $\chi_{\text{bulk}}$  for the rest of the Cu sites. In the  $^{17}\text{O}$  NMR experiments,<sup>7</sup> we then suggest four main groups of the oxygen Knight shifts as shown in Fig. 3. We hope that our finding and improved experimental resolution can be used to further test the applicability of the Heisenberg model to the Herbertsmithite.

In the low temperature study, we attempt to understand the susceptibility histograms in the spin liquid framework, taking up the ASL of Hastings<sup>24</sup> and Ran *et al.*<sup>25</sup> with Dirac spectrum for the spinons. First we perform the mean field analysis treating the spinons as free fermions hopping on Kagome lattice with impurity sites removed. Again we calculate the susceptibility near a single impurity and in the presence of 5% of impurities. We should say from the outset that such a simplified treatment of the spinons is likely inadequate near impurities and one should allow modifying both spinon hopping amplitudes and fluxes near impurities. For example, the exact diagonalization study<sup>33</sup> finds strong singlet correlations on bonds next to an impurity. Furthermore, thinking about possible more accurate self-consistent treatments suggests that the spinon hopping should also be strengthened on these bonds. Such modifications will

certainly have significant effect on the calculated susceptibility of the spins nearest to the impurity. However we argue that there are robust features in the susceptibility histograms that are insensitive to the details of the treatment near the impurities. The vacancies are a source of disorder which will induce a finite density of states at the Fermi level with a characteristic spatial distribution. The bulk susceptibility associated with the sites that are further from impurities decreases as the temperature is lowered, just as it would for the pure system where it goes all the way to zero because of the vanishing density of states at the Fermi energy in the Dirac spectrum. However the impurities cause finite density of states and as more and more sites start to feel the impurities as we lower the temperature, which all sites eventually do since there is a finite density of impurities, the movement of the histogram peak to zero stops as is seen in Fig. 7. There, the detailed features seen at high temperatures depend on the treatment of impurities and should not be taken quantitatively; on the other hand, the overall picture of the disorder-induced broadening of the vanishing pure Dirac susceptibility into an asymmetric histogram should be more robust.

We also test the approach beyond the mean field by studying the magnetization distribution in the trial spin wavefunctions obtained by Gutzwiller projection. This approach can reproduce nontrivial results for the local susceptibilities near impurities in one dimension.<sup>35</sup> In the Kagome system with impurities, the main effect that we find is the increase in local susceptibility variation by about a factor of two, while the qualitative predictions of the mean field remain unchanged. In particular, we find that the local susceptibility can be also negative, deviating significantly from the positive bulk value. This can happen because there are strong antiferromagnetic correlations in the system.

From the above discussion, it is clear that the local susceptibility variation due to impurities is significant both at high and low temperatures and its experimental observation can reveal a wealth of information about the spin state. At high temperatures, it is possible to track several features associated with different locations relative to impurities. In particular, the susceptibility at the oxygen sites next to impurity should be  $\chi_1$  which is different from the half of  $2\chi_{\text{bulk}}$  seen by the oxygens in the bulk. If one could improve NMR line resolution, more peaks should be observable at high temperatures. On the other hand, the peaks broaden as the temperature is lowered and particularly as the system enters the correlated paramagnet regime. Our spin liquid study suggests that there remain no features in the susceptibility histogram except for the overall peak associated with the bulk sites, which first moves towards zero as in the pure Dirac spin liquid and then stops because of the disorder-generated nonzero density of states at the Fermi level. This is reminiscent of what is observed in the  $^{17}\text{O}$  NMR experiments, even if not in every detail; it is also qualitatively different from the spin liquid with a Fermi surface,

where there is a finite density of states in the pure system and the impurities would only broaden the histogram both ways without changing significantly the bulk peak location.

## II. HIGH TEMPERATURE SERIES EXPANSION

We consider spin 1/2 nearest neighbor anti-ferromagnetic Heisenberg model on Kagome lattice. Local spin susceptibility at site  $i$  is given by

$$\chi_{\text{loc}}(i) = \frac{(g\mu_B)^2 \langle S_i^z S_{\text{tot}}^z \rangle}{k_B T}, \quad (1)$$

where  $S_{\text{tot}}^z = \sum_j S_j^z$ . We calculate  $\chi$ 's in the high temperature series expansions in the presence of a single nonmagnetic impurity, treated as a missing site (vacancy). We also study the Kagome system in the presence of a finite density of nonmagnetic impurities, which we chose to be 5% as motivated by experiments<sup>5,6,7</sup> in  $\text{ZnCu}_3(\text{OH})_6\text{Cl}_2$ .

The expansion is performed to the 12-th order in  $J$  (or 13-th order in  $1/T$ ) using the linked cluster expansion.<sup>36</sup> The outline of the procedure is as follows. We generate all abstract graphs up to desired size. Then we generate all subgraphs of these graphs, keeping track of the location of each subgraph in the graph. We calculate the local susceptibility for each graph at each point of the graph. Then we subtract all the subgraphs of each graph as needed in the linked cluster expansion to get the contribution this graph would give when embedded into lattice. The local susceptibility on any lattice can be calculated by creating all possible embeddings of all graphs and adding their contributions at every site. In this general formulation, the lattice does not need to be regular; in particular, this procedure applies to the Kagome lattice with impurities. In the practical implementation, we use the symmetries of the underlying pure Kagome lattice for efficiency and discard the embeddings that contain an impurity. In this way, we obtain exact  $1/T$  series for the system with impurities.

One more remark about the method. In the derivation of the linked cluster expansion for the local susceptibility, one needs to calculate expressions of the form  $\text{Tr}(H^a S_i^z H^b S_{\text{tot}}^z H^c)$  where  $a, b, c$  are integers. Since the total spin is conserved,  $[S_{\text{tot}}^z, H] = 0$ , and because of the cyclic property of the trace, this can always be written as  $\text{Tr}(H^{a+b+c} S_i^z S_{\text{tot}}^z)$ . Thus every diagram can be evaluated using this expression.

After obtaining the series, we extend it beyond the radius of convergence using the method of Pade approximants. We use [5,6], [5,7], [6,6], [6,7] and expand in variable  $1/(T + \alpha)$  where  $\alpha$  is usually 0.08 as in Ref. 37. Depending on  $\alpha$  one might get a pole in the expression, and hence divergence in susceptibility even at relatively large temperature. This usually happens say in one of the approximants while the others still overlap. At low enough

temperature they start diverging and we take that as a point where the approximation stops being valid. Different values of  $\alpha$  are tried, and sometimes it is possible to tune to a value where all the curves overlap completely to a much lower temperature, but that is a pathology, probably indicating that the polynomials are all the same. For other values of  $\alpha$  the curves usually start to diverge from each other at around the same temperature.

### A. Single Impurity

The series coefficients of the pure Kagome lattice susceptibility and of the local susceptibilities of the first four nearest neighbors near a single impurity are in Table I. The corresponding susceptibilities are plotted in Figure 1.

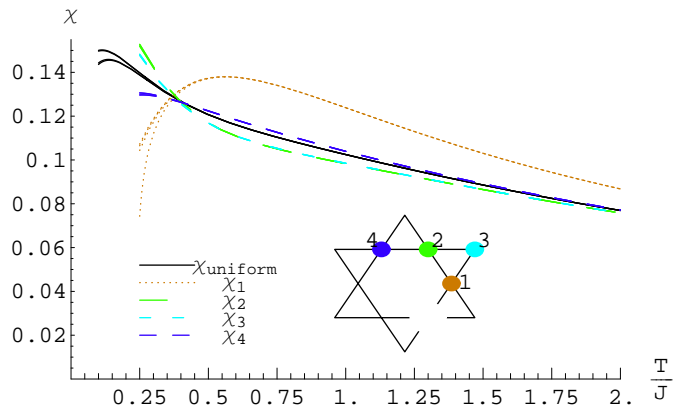


FIG. 1: [Color Online] Susceptibility of the pure Kagome system (far from any impurities) and local susceptibilities at the first four inequivalent neighbors of a nonmagnetic impurity. For each  $\chi_i$ , there are actually four curves of the same color corresponding to the Pade approximants [5,6], [5,7], [6,6], [6,7]; the plotting is cut where these curves start to diverge from each other. The  $\chi_2$  and  $\chi_3$  happen to overlap over the entire temperature range shown.  $\chi$  is in units  $(g\mu_B)^2/J$ .

From Fig. 1, we see that for the temperatures  $T \gtrsim 0.3J$ , only the first few neighbors – most visibly the  $\chi_1$  right next to the impurity – deviate significantly from the susceptibility of the clean system. The  $\chi_1$  is about 15-20% larger than  $\chi_{\text{uniform}}$  over a wide temperature range  $0.5J \lesssim T \lesssim 2J$ . As the temperature is lowered further, the  $\chi_1$  starts to decrease while the  $\chi_{\text{uniform}}$  still grows, and we see  $\chi_1$  dropping below  $\chi_{\text{uniform}}$ . This is reminiscent of the picture in the exact diagonalization study in Ref. 33, in which a pair of spins in the same triangle as the impurity (there are two such triangles) forms a singlet at low temperatures, and therefore the susceptibility of these spins is strongly reduced.

TABLE I: Series coefficients  $a_n$  of  $\chi = \frac{g^2 \mu_B^2}{T} \sum_{n=0} \frac{a_n}{4^{n+1}(n+1)!} (\frac{J}{T})^n$  for susceptibility  $\chi_{\text{uniform}}$  of the pure Kagome lattice and for the four closest neighbors  $\chi_i$  of nonmagnetic impurity as indicated in Figure 1. The coefficients for the uniform susceptibility agree with Ref. 16 except for  $n = 6$ , which is probably a typo there.

n	$\chi_{\text{uniform}}$	$\chi_1$	$\chi_2$	$\chi_3$	$\chi_4$
0	1	1	1	1	1
1	-8	-6	-8	-8	-8
2	48	30	42	42	48
3	-96	-120	-8	-8	-48
4	-320	680	-360	-240	-1360
5	-38784	-14592	-45264	-47424	-40512
6	677824	158144	540624	465248	995680
7	14176256	2843520	16451456	18525184	15092736
8	-429202944	-57813120	-312132096	-249716736	-636643584
9	-11927946240	-2620491520	-12841824000	-15158219520	-12108702720
10	501186768896	64507410176	346403354880	271966979328	700664177664
11	13960931721216	3019001330688	14456058461184	17966636077056	13440259983360
12	-841802086780928	-98970319958016	-558124102202368	-437482821907456	-1111015315910656

## B. 5% Density of Impurities

We take a  $60 \times 60 \times 3$  Kagome lattice with periodic boundary conditions and 540 randomly placed impurities (corresponding to 5% density). By considering all possible abstract graph embeddings in the finite system, we calculate exact  $1/T$  series for the local susceptibilities in the sample. Analyzing these as before, we obtain reliable quantitative results down to about  $T = 0.5J$ . The local susceptibility histograms for several temperatures are shown in Figure 2. We also calculate the susceptibilities at the oxygen atom sites that the experiments measure; the corresponding histograms are displayed in Fig. 3.

The sample is sufficiently large that the obtained histograms are accurate representations of an infinite system; in particular, all features seen in Fig. 2 are real. The peaks are not delta functions because all sites feel the impurities, and the different peaks correspond to different locations relative to one or several impurities. We estimated the errors by dividing the sample into ten pieces, getting the histogram for each, and calculating deviations from the average. The resulting relative error on the  $y$  axis in Fig. 2 is roughly 5%. There is also a systematic error along the  $x$  axis coming from the truncated series and the Pade approximants, but from the single impurity study we believe the results are reliable for the temperatures shown.

To the first approximation, we can say that there are two major groups of sites: one is the sites next to impurities (susceptibilities in the histogram near  $\chi_1$ ), and the other is the rest of the sites (susceptibilities near  $\chi_{\text{bulk}}$ ). In the second group, we can also clearly see a subgroup formed by the sites that are second neighbors to some impurity and have susceptibilities near  $\chi_2, \chi_3$ .

Turning to the  $^{17}\text{O}$  NMR experiments, each oxygen can

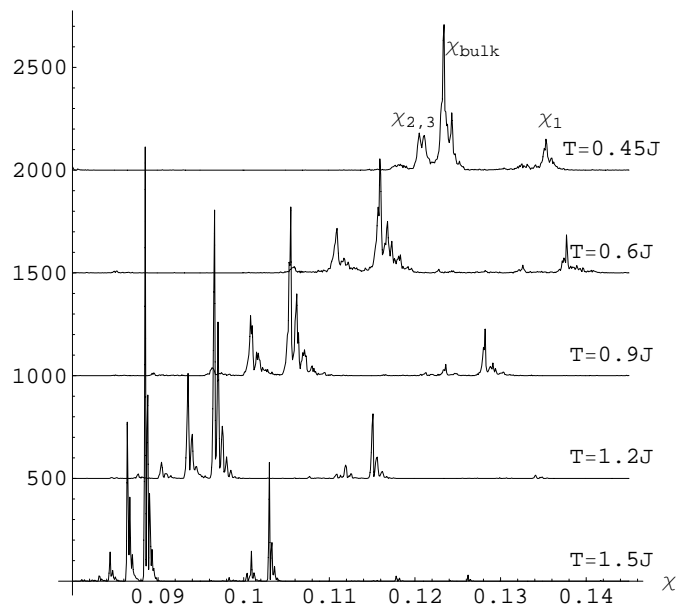


FIG. 2: Histogram of local susceptibilities at the sites of Kagome lattice in the presence of 5% of nonmagnetic impurities. Pade approximant [6,6] was used to analyze exact series at each site of a large but finite  $60 \times 60 \times 3$  sample with randomly placed impurities.  $\chi$  is in units  $(g\mu_B)^2/J$ .

be associated with a bond  $\langle ij \rangle$  of the Kagome lattice and feels only these two sites  $i$  and  $j$ . The appropriate histogram of such  $\chi_i + \chi_j$  is in Figure 3.

In the first approximation, we see four major groups of peaks which can be roughly identified as follows. Imagine that only the susceptibility of the sites next to the

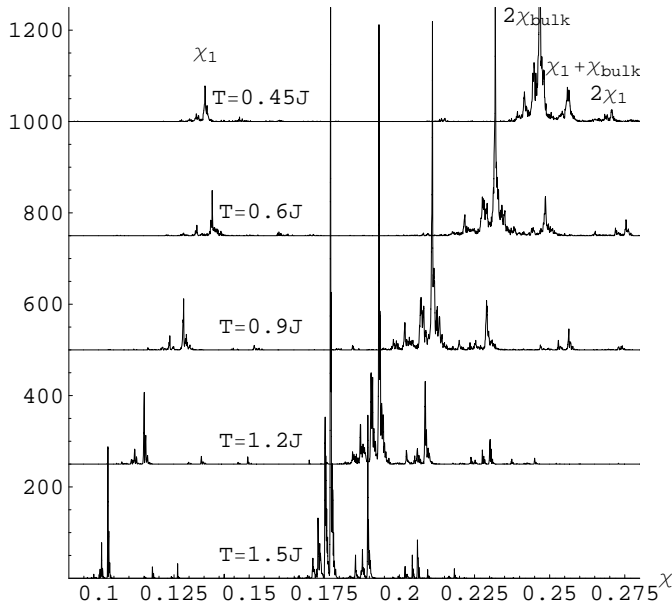


FIG. 3: Histogram of the susceptibilities at oxygen sites in the presence of 5% of nonmagnetic impurities. The system is the same as in Fig. 2 and we used the same Pade approximant [6,6].

impurities is modified and is  $\chi_1$ , while the rest of the Cu sites have  $\chi_{\text{bulk}}$  (in particular we join the  $\chi_2$  and  $\chi_3$  with the  $\chi_{\text{bulk}}$ , even though they are still separately visible in Fig. 2). The leftmost peak in Fig. 3 is located near  $\chi_1$  and comes from the oxygens next to impurity that feel only one Cu site, and so the value is roughly half compared to all other oxygens. The dominant peak is near  $2\chi_{\text{bulk}}$  and comes from oxygens that are in the bulk - neither near impurity, nor near Cu next to impurity. The rightmost peak is located around  $2\chi_1$  and comes from oxygens that are interacting with two Cu sites that are next to impurity. Finally, the group  $\chi_1 + \chi_{\text{bulk}}$  comes from oxygens that are interacting with one site near and one not near impurity. Again, the finer features and the finite widths of the peaks originate from the variation of the susceptibility with the distance from various impurities a given site feels. The volume fractions of the four groups of peaks in Fig. 3 say at  $T = 0.6J$ , are, from the left, roughly 8%, 70%, 15%, 5%. If we calculate how many oxygens of each type other than  $2\chi_{\text{bulk}}$  are near a single impurity and then multiply it by the density of impurities and divide by the ratio of the number of oxygens to the number of Kagome sites (two), we would get the following percentages 10%, 65%, 20%, 5%; these are slightly different from the exact numbers because some sites are close to more than one impurity.

Thinking about the experiments, the NMR lines are too broad to resolve the groups  $2\chi_{\text{bulk}}$ ,  $\chi_1 + \chi_{\text{bulk}}$ , and  $2\chi_1$ , but just enough to separate these from the group

$\chi_1$ . We hope that our study will stimulate further NMR experiments with more site resolution.

### III. DIRAC SPIN LIQUID: MEAN FIELD WITH IMPURITIES

In this section we explore the Kagome system with non-magnetic impurities at low temperatures within a particular spin liquid proposal of Hastings<sup>24</sup> and Ran *et al.*<sup>25</sup>. In the clean system, one has fermionic spinons hopping on the Kagome lattice in the presence of  $\pi$  flux through every hexagon. Ran *et al.*<sup>25</sup> showed that the corresponding spin wavefunction obtained by Gutzwiller projection has very good variational energy.<sup>25</sup> Again we consider the cases of a single impurity and 5% density of impurities. We take a crude model of the spin liquid in the presence of impurities by simply removing the vacancy sites (and the links) in the spinon hopping problem. We will argue that while this is not fully adequate, particularly for detailed features near impurities, the results for the overall behavior of the bulk of the local susceptibility histograms are robust. We will further discuss possible improvements of our approximation in Sec. III D.

In the mean field the fermions are free. The spectrum of the clean system has a flat band at the lowest energy containing 1/3 of states with gap to the next band. The system has Dirac points at fillings 1/2, 2/3 and 5/6. In our approach, adding impurities does not destroy the flat band (which can be expressed in terms of localized states), but also produces localized states in the gap. For a finite concentration of impurities, which is our main interest, the Dirac points are filled with finite density of states (DOS). We consider the system at half filling which corresponds to spin 1/2. The pure system has Dirac nodes and a linearly vanishing density of states at the Fermi level, while the impurities induce a finite density of states, and one of the main questions we address is how it is distributed locally.

If  $\{\psi_n(i)\}$  is the set of single-particle wavefunctions, it is easy to show that the local susceptibility at temperature  $T$  is given by

$$\chi_{\text{loc}}(i) = \frac{(g\mu_B)^2}{2T} \sum_n |\psi_n(i)|^2 f(\epsilon_n)(1 - f(\epsilon_n)) \quad (2)$$

where  $f(\epsilon) = 1/(e^{(\epsilon-\mu)/T} + 1)$  is the Fermi distribution. For a given configuration of impurities, we obtain the single-particle orbitals by numerical diagonalization and use this formula to calculate the local susceptibility. In the  $T \rightarrow 0$  limit, the local susceptibility is simply proportional to the local density of states at the Fermi level,  $\nu_{\text{loc}}(i) = \sum_n |\psi_n(i)|^2 \delta(\epsilon_n - \mu)$ .

Let us briefly describe the localization properties of the single-particle states in our system with 5% density of impurities. We expect that all states are eventually localized, since this is a time-reversal invariant Anderson

localization problem in two dimensions with no special symmetries. The localization is weaker in the spectral regions where the density of states is high and is stronger where the DOS is low, e.g., in the vicinity of the Dirac nodes of the pure spectrum. However, even for the latter as happens around half-filling, the localization lengths are still very large. For example, we calculate the participation ratios of the states near half-filling and find that the corresponding volume fraction of participating sites decreases only from about 14% in a  $30 \times 30 \times 3$  system to about 10% in a  $60 \times 60 \times 3$  system, indicating that these states are still extended over our system sizes up to  $60 \times 60 \times 3$ . On the other hand, such long distance localization physics does not affect our measurements of local properties at finite temperatures presented here. For example, even a single disorder sample in a system as small as  $10 \times 10 \times 3$  produces the susceptibility histogram which is essentially the same as from much larger samples.

Some explanations are in order before we show the results for the local susceptibilities. Throughout, we keep the spinon hopping  $t$  fixed and vary the temperature. All presented susceptibilities are in units of  $(g\mu_B)^2/t$ . In a more realistic calculation, the spinon hopping would need to be found self-consistently for a given Heisenberg exchange  $J$  and temperature  $T$ . In such treatments of pure systems, one typically finds that the self-consistent  $t$  vanishes above some temperature of order  $J$  (e.g., in the renormalized mean field scheme this temperature is  $0.75J$ ). There is no sense of speaking about spinons above this temperature, and the system is more appropriately described in terms of weakly correlated individual spins. On the other hand,  $t$  becomes nonzero at lower temperatures, suggesting that the system enters the correlated paramagnet regime. Below the onset temperature, the self-consistent  $t$  quickly reaches the values similar to the zero-temperature limit. It is this regime where  $t(T) \simeq t(T=0)$  that we are describing.

We can estimate the spinon hopping amplitude from self-consistent mean field conditions. For example, in the so-called renormalized mean field scheme, this reads

$$t_{ij} = \frac{3g_s J_{ij}}{8} \langle f_{j\sigma}^\dagger f_{i\sigma} \rangle, \quad (3)$$

where  $g_s$  is some renormalization factor (which can be found, e.g., by comparing measurements before and after the projection). In the case with  $\pi$  flux through each hexagon and at  $T=0$ , Hastings found  $|\langle f_{j\sigma}^\dagger f_{i\sigma} \rangle| = 2 \cdot 0.221$ . Using a reasonable  $g_s = 4$ , we then find  $t = 0.66J$ . On the other hand, from the study of the projected wavefunctions, Ran *et al.*<sup>25</sup> suggest

$$t \approx 0.4J \approx 70K. \quad (4)$$

These are crude but reasonable estimates of the spinon band energy scales.

## A. Pure System and System with a Single Impurity

As mentioned, the local susceptibility near an impurity depends strongly on how the spin liquid is modified near this impurity. However, for illustration, we show the local susceptibility of the first few neighbors for the case where we simply remove the appropriate links from the fermion hopping problem. For the size  $44 \times 44 \times 3$  this is shown in Fig. 4. The susceptibilities vanish linearly when  $T \rightarrow 0$ , since the pure system is perturbed only by a single impurity here. In our approximation, the susceptibility  $\chi_1$  of the site next to the impurity is larger than the bulk susceptibility. This happens because we take all bonds to have the same strength, while the  $\chi_1$  sites have fewer bonds. This is an example where we believe the simplified treatment near the impurity is inadequate and the  $\chi_1$  results should not be taken seriously. A more accurate self-consistent treatment would likely require a stronger hopping amplitude connecting two such sites next to an impurity, and this would decrease  $\chi_1$ . We discuss such possible improvements over the current treatment in Sec. III D.

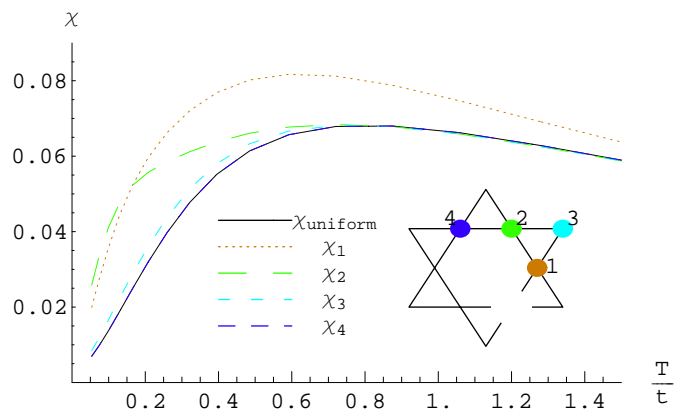


FIG. 4: [Color Online] The susceptibilities of first few neighbors near single impurity in the spin liquid with  $\pi$  fluxes through each hexagon on Kagome lattice.  $\chi$  is in units  $(g\mu_B)^2/t$ .

We also plot the shape of local susceptibility near a single impurity in Figure 5. The “ringing” that we see is a more universal aspect of the Knight shift texture around the impurity. The corresponding wavevectors are the mid-points of the Brillouin zone edges and are characteristic for this spin liquid. One can obtain some analytic understanding of the mean field results by working perturbatively in the non-magnetic impurity strength. One finds that  $(\chi_{\text{loc}} - \bar{\chi})/\bar{\chi}$  decays away from the impurity with a  $1/r$  envelope on length scales  $1 \ll r \ll v/T$  and exponentially on larger scales (here  $v$  is the Fermi velocity, and we referenced  $\chi_{\text{loc}}$  by  $\bar{\chi}$  remembering that the susceptibilities vanish in the  $T \rightarrow 0$  limit).

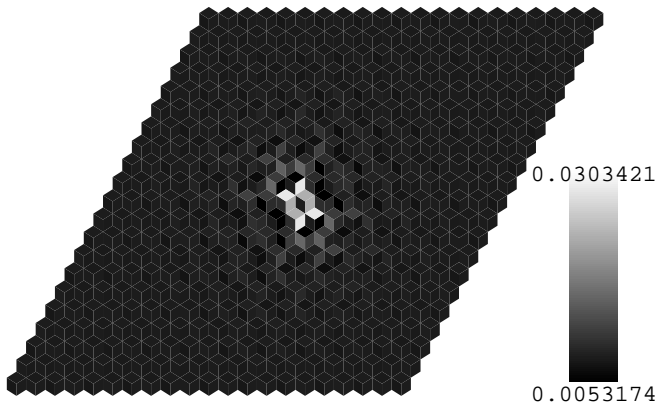


FIG. 5: The susceptibilities near single impurity in the spin liquid with  $\pi$  fluxes through each hexagon on Kagome lattice at temperature  $T = 0.054t$  where  $t$  is the hopping amplitude. In this figure, the color of a given point in the plane is given by the value at the nearest Kagome site.

### B. 5% Density of Impurities

For the system with 5% density of impurities, the histogram of local susceptibilities at Kagome (Cu) sites is in Figure 6 and at oxygen sites in Figure 7.

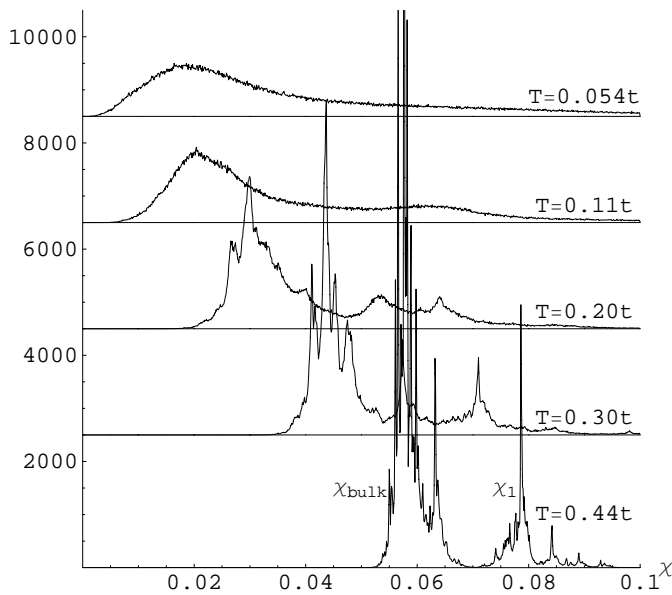


FIG. 6: The histogram of susceptibilities on the Kagome lattice sites in the spin liquid of fermionic spinons with  $\pi$  fluxes through hexagons in the presence of 5% of impurities, treated by simply removing the sites from the spinon hopping problem. The histogram is the average of 300 samples of size  $20 \times 20 \times 3$ .  $\chi$  is in units  $(g\mu_B)^2/t$ .

We can understand the main features in the  $\chi_{loc}$  his-

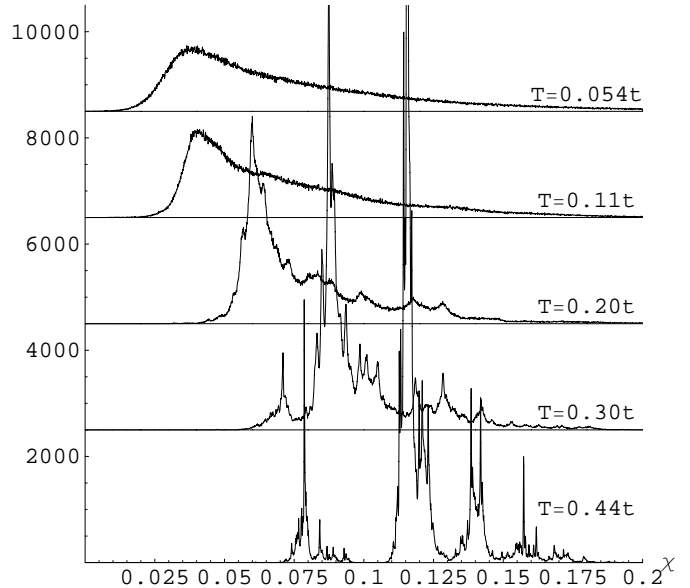


FIG. 7: The histogram of susceptibilities on oxygen sites in the spin liquid in the presence of 5% of impurities. The systems is the same as in Fig. 6. The histogram is the average of 300 samples of size  $20 \times 20 \times 3$ .

tograms as follows. At the highest temperature shown,  $T = 0.44t$ , there are two main groups, just as in the high temperature series analysis. The group with the higher  $\chi$  comes from the sites that are next to the impurities, while the other with the lower  $\chi$  comes from the rest of the sites (bulk) and contains the main weight of the sites. As the temperature is lowered, the two features move towards smaller susceptibilities, but the bulk one moves faster. Also, between  $T = 0.4t$  and  $T = 0.2t$ , we see a new feature splitting away from the bulk and moving slower; we can roughly identify this feature with the sites that have impurities as their second neighbors. The continuing marching of the bulk sites that are further from the impurities to smaller  $\chi$  is what the clean Kagome lattice would do because of the vanishing density of states, see Fig. 4. As we lower the temperature, however, the influence of the impurities spreads to further and further neighbors, and the local susceptibility at the sites that already feel the impurities starts to slow down and eventually saturates at a finite local  $\chi$ .

At  $T = 0.1t$ , we already see no sharp features associated with specific locations away from an impurity since all the sites already feel many impurities. The broad peak corresponds to the “bulk” sites that are furthest from impurities; it remains visible since this group of sites contains the largest volume fraction among the successive “layers” around impurities. The bulk peak stops its motion below  $T = 0.1t$ ; its eventual location corresponds roughly to the typical impurity-induced local

density of states at these bulk sites. Note that this value  $\chi_{\text{peak}} \approx 0.02/t$  is about two times smaller than the average over all sites  $\bar{\chi} = 0.0425/t$ ; the latter contains contributions from the sites close to impurities where the induced density of states is typically larger.

This behavior of the bulk peak is our main and robust prediction. On the other hand, the behavior of the other peaks visible at high temperatures depends on specific details of the treatment of the impurity; these features should not be trusted in our simplified approach and we will discuss the ways to improve the treatment in Section III D.

Thinking about the NMR experiments, the bulk peak susceptibility at low temperatures  $\chi_{\text{peak}} \approx 0.02/t \sim 0.04/J$ , where we used Eq. (4). This is about one half of the bulk spin susceptibility at  $T = 2J$  from the high temperature series study, Fig. 1. In the  $^{17}\text{O}$  NMR experiments, this ratio is between one half and one third, so our spin liquid results are reasonable.

To conclude this section, let us see if the disorder-induced density of states can give sensible thermodynamic properties in the Herbertsmithite. In our treatment with 5% impurity concentration, the DOS at the Fermi level is

$$\nu(\epsilon_F) = 0.085/t \quad (5)$$

per site per single spin species. This would give average spin susceptibility of the Cu in the Kagome layer

$$\bar{\chi} = 2\nu(\epsilon_F)\mu_B^2 = 6.4 \cdot 10^{-4} \times \left(\frac{100\text{K}}{t}\right) \frac{\text{emu}}{\text{mol Cu}}. \quad (6)$$

One should not take these numbers literally, since  $\nu(\epsilon_F)$  depends quantitatively on the treatment near impurities, which is very crude here. Still, an estimate of  $t$  like that in Eq. (4) produces  $\bar{\chi} \sim 10^{-3}$  emu/mol Cu that compares reasonably with the experimental estimate of the intrinsic Kagome layer susceptibility in Ref. 5. Furthermore, in the mean field treatment, spinons will contribute to the specific heat as

$$c_v = 2\nu(\epsilon_F)\frac{\pi^2}{3}k_B^2T = 4.6 \times \frac{k_B T}{t} \frac{\text{Joule}}{\text{K} \cdot \text{mol Cu}}. \quad (7)$$

which again yields reasonable numbers for temperatures of several Kelvin.<sup>1,5</sup>

### C. Gutzwiller Wavefunction Study of the Local Magnetizations

In this section, we pursue the spin liquid proposal one step beyond the mean field. For the slave fermion approaches, one can achieve this by performing the Gutzwiller projection of the singlet mean field state into the space with precisely one fermion per site. This approach is appealing since one obtains a physical spin wavefunction, which can be viewed as a variational state

for an energetics study (and one can also study properties of this spin state). As we have already mentioned, Ran *et al.*<sup>25</sup> performed the energetics study of the clean Kagome system and found the discussed  $\pi$ -hexagon spin liquid to have the lowest trial energy. We expect that the same construction on a lattice with vacancies will have good energetics also for small concentration of impurities. It is interesting to explore this issue in more detail in the future, and we comment on this in Sec. III D below, while here we want to take a crude look whether such proposal can explain the observed inhomogeneous Knight shifts in the Herbertsmithite.<sup>3,7</sup> The specific results that we find here are as follows. The spin susceptibilities are always positive in the mean field. We show that they can become negative and the Knight shift distributions are actually broader when we go beyond the mean field.

Unfortunately, one can not access the local susceptibilities from the study of the singlet ground state. To circumvent this, we consider trial states with non-zero  $S_{\text{tot}}^z$  and study how the total spin is distributed among the lattice sites. The idea is that the pattern of the local magnetizations  $m_i^z = \langle S_i^z \rangle$  in such weakly polarized states is similar to that of the local susceptibilities at low temperatures. This approach has been used in exact diagonalization studies of spin systems with impurities, where one considers  $m_i^z$  in the lowest-energy states in the sectors with nonzero  $S_{\text{tot}}^z$ . We are trying this in the variational spin liquid studies in the present Kagome problem and also for the organic spin liquid on the triangular lattice.<sup>38</sup> (We have also tried this approach in a one-dimensional chain with vacancies<sup>39</sup> and reproduced the non-trivial qualitative behavior predicted by Eggert and Affleck.<sup>35</sup>)

Consider a mean field state with different chemical potentials for the two spin species,  $\mu_{\downarrow} < \mu_{\uparrow}$ . The orbitals with  $\mu_{\downarrow} < \epsilon < \mu_{\uparrow}$  are occupied by the  $\uparrow$  spins but not by the  $\downarrow$  spins, which produces non-zero  $S_{\text{tot}}^z = (N_{\uparrow} - N_{\downarrow})/2$ . In the mean field, the local magnetization is given by

$$m_{\text{loc}}(i) = \frac{1}{2} \sum_{\mu_{\downarrow} < \epsilon_n < \mu_{\uparrow}} |\psi_n(i)|^2. \quad (8)$$

Observe the similarity of this expression to that for the local susceptibility at finite temperature, Eq. (2). The difference is that here the contributing orbitals are selected by a sharp energy window  $[\mu_{\downarrow}, \mu_{\uparrow}]$ , while in Eq. (2) the window is soft proportional to  $(-\partial f/\partial \epsilon)$  with width set by the temperature. If there is a finite density of states at the Fermi level and if the properties of the orbitals do not change strongly with the energy, the two windows of similar width should give similar results for the local magnetization or susceptibility normalized by the corresponding average values. The above two windows roughly match when  $\mu_{\uparrow} - \mu_{\downarrow} \approx 4T$ . In our numerical calculations, we indeed observe such correspondence of the  $m_{\text{loc}}$  and  $\chi_{\text{loc}}$  distributions.

From the mean field state with non-zero  $S_{\text{tot}}^z$ , we construct the spin wave function by Gutzwiller projection.



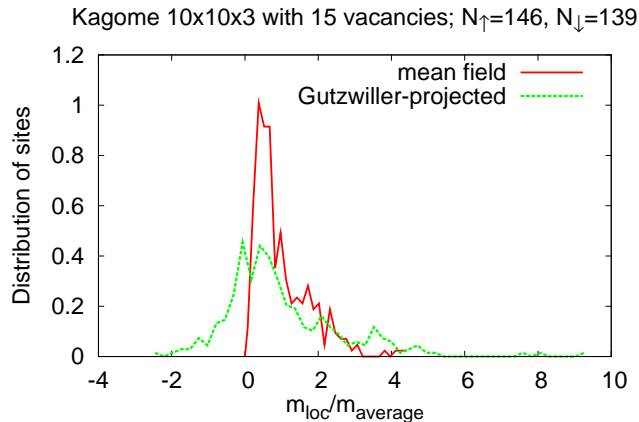


FIG. 8: [Color Online] Distribution of the local magnetization in the  $\pi$ -flux spin liquid state with non-zero  $S_{\text{tot}}^z$ . The sample is  $10 \times 10 \times 3$  with 15 randomly placed vacancies; the total magnetization is  $S_{\text{tot}}^z = (N_{\uparrow} - N_{\downarrow})/2 = 7/2$ . We compare the mean field and the Gutzwiller-projected results for exactly the same system and find that the projection broadens the histogram by about a factor of 1.5-2, which can be clearly seen despite the noisiness of the data in the single random sample.

Note that  $S_{\text{tot}}^z$  is preserved by the projection, so the average magnetization is unchanged. However, the local magnetizations are modified. Our observations in the present system can be summarized by the following crude rule: The deviation of the site magnetization from the average is enhanced by the projection by a typical factor between 1.5 and 2. This implies that the distribution of the local magnetization is broadened by the same factor upon the projection. Figure 8 illustrates this for a  $10 \times 10 \times 3$  sample with 15 vacancies and  $N_{\uparrow} - N_{\downarrow} = 7$ .

We have tried several lattice sizes, different disorder samples, and different magnetizations  $S_{\text{tot}}^z = (N_{\uparrow} - N_{\downarrow})/2$ , and in all cases observed the above rule. This rule is not strict but holds for a majority of sites. More precisely, the histogram of the ratios  $(m_{\text{loc}}^{\text{Gutzw}} - \bar{m}) / (m_{\text{loc}}^{\text{meanfield}} - \bar{m})$  is peaked near 1.5 – 2, which is the claimed typical enhancement factor for the deviations from the average. In particular, while the mean field local magnetization is always non-negative, see Eq. (8), the local magnetization can become negative after the projection. It can be opposite to the bulk magnetization because of the antiferromagnetic correlations present in the system.

Let us say few words about our choice of  $N_{\uparrow}, N_{\downarrow}$  in Fig. 8. On one hand, if we take  $N_{\uparrow} - N_{\downarrow} = 1$ , we worry if the results are dominated by the specific single-particle state that happened to lie at the Fermi level. This is a concern because of our view that all states will be eventually Anderson-localized. However, by considering the participation ratio for the states near the Fermi level in the present sample, we find that they are still spread over about one third of the sites. We have

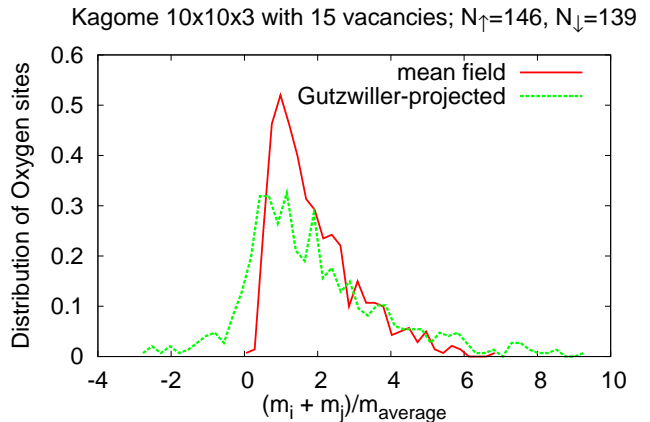


FIG. 9: [Color Online] Oxygen NMR local fields corresponding to the same system as in Fig. 8.

checked that even for such small  $N_{\uparrow} - N_{\downarrow}$  the results for the broadening of the distribution by the projection are qualitatively similar. On the other hand, we do not want  $N_{\uparrow} - N_{\downarrow}$  to be large, which could take us far from the region in the spectrum near the Fermi level and also would correspond to physically inaccessible magnetization. Our  $N_{\uparrow} = 146, N_{\downarrow} = 139$  is a compromise, since a few typical states around the Fermi level are sampled, and also since it corresponds to about 2.5% of the maximal polarization, which is reasonable also from the experimental perspective. For example, using the estimate<sup>6</sup>  $\chi_{\text{intrinsic}} = 1.25 \cdot 10^{-3}$  emu/mol Cu, the field of 7 Tesla in the  $^{17}\text{O}$  experiments<sup>7</sup> magnetizes the system to about 1.5% of the maximal polarization of the Kagome layer.

To conclude this section, we find that the Gutzwiller trial wavefunction treatment does not modify the mean field results qualitatively but widens the magnetization distributions by about a factor of two.<sup>40</sup> In particular, at low temperature the distribution will have a sizable wing on the negative values, which is consistent with the NMR experiments.<sup>3,7</sup> To describe the  $^{17}\text{O}$  NMR line, we need to histogram the field  $m_i + m_j$  associated with bonds  $\langle ij \rangle$  of the Kagome lattice. This is shown in Fig. 9. The wing at negative fields is weaker than in the Cu NMR because the oxygens perform some “averaging” of the local  $m_i$  (while the total magnetization is positive). We reiterate here the crudeness of our study; in particular, we are not attempting here to explain the actual experimental histogram in the  $^{17}\text{O}$  NMR, which looks nearly symmetric with respect to the peak at the lowest temperature. Our main message is that within the spin liquid approach, by going beyond the mean field, we expect broader distribution of the Knight shifts with both positive and negative susceptibilities due to the underlying correlations.

#### D. Issues with the Spin Liquid Treatment and Possible Improvements

The main reservation about the presented spin liquid study is that we modeled the effect of impurities by simply removing the Zn sites in the spinon mean field. We did not perform a self-consistent mean field or an energetics study of the system with impurities. However, we did think how such more accurate treatments could affect our results and tested the robustness of the features by trying different modifications that such treatments might require.

One minor concern is that even though the system is inhomogeneous, we require the half-filling for spinons only on average over the whole sample and not at each site. The latter is likely a better treatment since then the Gutzwiller projection is less drastic and the mean field is closer to the projected state. We find that in our samples the deviations of the local densities from the average are small and smaller in relative terms than the deviations of the local susceptibilities that we are interested in. We also tested small systems achieving the half-filling precisely at all sites by adjusting local chemical potential and found that the susceptibilities did not change qualitatively or significantly quantitatively and only at the the lowest temperatures the histograms became somewhat broader.

A more serious concern is that we took the spinon hopping amplitudes to be the same as in the clean system, instead of finding them self-consistently. Thus, we expect that at low temperatures the hopping connecting two sites that are both next to an impurity should be larger than for other bonds. Consider, for example, the renormalized mean field scheme, Eq. (3). When we calculate the bond expectation value  $\zeta_{ij} = \langle f_j^\dagger f_i \rangle$  in our mean field starting with all  $t_{ij}$  equal, which can be viewed as a first step in the self-consistency iteration, we find that it is the largest on the bonds next to impurities. We have not pursued this scheme any further since in the present case it would actually lead to a dimer state in the clean system, which we know is a pathology of such treatment when applied to the spin-1/2 system. Roughly, one should not be using the same renormalization factor  $g_s$  irrespective of the bond expectation value. By comparing with the Gutzwiller-projected measurements, one typically uses  $g_s = 4$  for translationally invariant states, but one should take a smaller  $g_s = 2$  for the dimer states. One could use a different mean field scheme to capture this, e.g., the scheme due to Hsu,<sup>24,41</sup> which leads to the self-consistency conditions of the form

$$t_{ij} = \frac{3J_{ij}\zeta_{ij}(1 - 16|\zeta_{ij}|^4)}{(1 + 16|\zeta_{ij}|^4)^2}. \quad (9)$$

This suppresses the dimerization tendency of the less elaborate mean field but may be doing it already too much, while we may want to retain some possibility of local dimers in the system with impurities. We leave a detailed exploration of such approaches and whether they

can capture the actual energetics in the system with impurities to future work.

It is interesting to notice however that if we took the most naive treatment Fig. 4, at low enough temperatures the nearest neighbor susceptibility is larger than twice the bulk and a little peak starts to emerge on the right of the bulk peak in Fig. 7 for  $T \approx 0.11t$ . If this were the case then the peaks in Ref. 7 at low temperatures would have the opposite interpretation – bulk peak would become closer to zero and the next to impurity oxygen peak further from zero. However we cannot make this conclusion at this point since the bonding of the spins next to the impurity will decrease the local susceptibility near the impurity. We only would like to point out that one should be careful when interpreting the experiment.

For the treatment of the spin liquid near impurity, we only note some crude things that we tried to see how our results might be affected. Motivated by the above observation, we have studied local susceptibilities at low temperatures when we multiplied by 2 all the bonds connecting the two sites that are both next to an impurity. Certainly, this has a strong effect on the susceptibility  $\chi_1$  of these sites – it in fact becomes smaller than the bulk one, which is opposite to the results in the preceding section where the  $\chi_1$  is the largest. Thus, such treatment can make the results for  $\chi_1$  more in line with the series study, Sec. II, and exact diagonalization study, Ref. 33, that suggest that this susceptibility is depressed at low temperatures. On the other hand, the above change of the hopping strengths near impurities does not have significant effect on the bulk susceptibility histogram peak and its marching to lower values with decreasing temperature (except, of course, for small numerical differences). We have also tried modifying not only the strengths of the bonds but also fluxes next to impurities. For example, if we view the proposed  $\pi$ -hexagon spin liquid as a time reversal invariant way of performing flux attachment and flux-smearing mean field, obtaining Dirac spin liquid instead of a chiral spin liquid (see discussion in Sec. IIC of Ref. 42), it suggests that we should also remove a  $\pi$  flux when we remove a spin. In an exploratory Gutzwiller energetics study with impurities, we indeed find that this often improves the trial energy. As far as we are concerned here with the local susceptibilities, such local flux modification of course has an effect on the sites near the impurities, but has little effect on the described qualitative behavior of the bulk peak.

We also remark that making all hexagon fluxes equal to zero<sup>27</sup> results in a qualitatively different behavior of the bulk of the susceptibility histogram. Here the clean system has a finite density of states at the Fermi level and therefore a nonzero susceptibility at low temperatures. We tried this for the system with 5% density of impurities and indeed found that the bulk peak doesn't march down. Instead, it approaches a relatively large value of susceptibility and broadens to both high and low values of susceptibility. We then propose that the experiments suggest more a Dirac-like spin liquid than the one with

a full Fermi surface.

#### IV. CONCLUSIONS

Using the high temperature series expansion, we calculated local susceptibility for the nearest neighbor Heisenberg antiferromagnet on Kagome lattice down to about  $T \approx 0.4J$ . The resulting histogram of susceptibilities can be directly compared to the experiment to test whether the Heisenberg model with impurities applies to  $\text{ZnCu}_3(\text{OH})_6\text{Cl}_2$ . The calculated histogram contains a lot of fine structure some of which we hope can be observed if the resolution of the experiments improves. One issue not considered in experiments is that the local susceptibility  $\chi_1$  next to impurities is larger than the bulk value by as much as 20% at high temperatures between  $0.5J$  and  $2J$ . This should affect the peak associated with the oxygens close to impurity, and one should be careful at interpreting the observed features at the intermediate and lower temperatures. Our work suggests that  $\chi_1$  drops below the bulk value at low temperatures and is consistent with earlier exact diagonalization study<sup>33</sup> which found that these sites tend to form singlets. The latter was invoked in Ref. 7 to explain a sharp feature in the NMR signal appearing near low temperatures. This is appealing, but more work needs to be done to understand the origin of this feature, particularly in the presence of the sizable impurity concentration, and also with the added bulk peak contribution that we expect in the spin liquid regime.

At low temperatures we assumed that the system forms a spin liquid of Ran *et al.*<sup>25</sup> We calculated the susceptibility histograms in the mean field theory and went beyond mean field by using Gutzwiller projection. Our results for the local susceptibility should not be trusted quantitatively close to impurity, since these depend on the details of the treatment of the spin liquid near the impurities, while we took a crude approach and only outlined how one can make it more accurate. In particular, we are not able to discuss histogram features associated with sites close to impurities. However we have a robust prediction for the behavior of the peak coming from the bulk of the sites (Fig. 6): The bulk peak marches down with decreasing temperature; its weight is gradually spread as further layers of sites around the impurities start to feel their share of the impurity-induced density of states; the

broadening saturates when all sites start to feel several and more impurities. We expect this qualitative description to be insensitive to the details of the mean field in the immediate vicinity of the impurities. It is sufficient to know that the clean spin liquid has Dirac density of states and that the bulk sites do not see the impurities down to some temperature scale, while any treatment near the impurities represents some local disorder that always induces some density of states at the bulk sites. The effect of the Gutzwiller projection is crudely to increase the variation of the local susceptibility by about a factor of two. In particular, as the peak spreads some of the susceptibilities become negative.

This behavior is consistent with the observed Knight shifts in the  $\text{ZnCu}_3(\text{OH})_6\text{Cl}_2$  experiments. Such behavior observed in the presence of a sizable density of impurities then suggests that the clean spin liquid would have a vanishing density of states at the Fermi level. Thus it distinguishes this spin liquid from the proposal with a spinon Fermi surface for which the peak would not march down but instead saturate at a large positive value. On the other hand, since the Algebraic Vortex Liquid of Ryu *et al.*<sup>28</sup> has Dirac-like gapless character, it would likely produce inhomogeneous Knight shift behavior similar to the Dirac spin liquid.

In the future work it would be good to treat the spin liquid right near impurities more accurately, e.g., in a self-consistent mean field or in an energetics study, and consequently make a reliable prediction for the spin susceptibility at these sites. Quantitative comparison with other approaches such as exact diagonalization would also be useful. It would be interesting to consider quantitatively the gauge theory description of such spin liquid with disorder-induced finite density of states, though we do not expect our mean field results to be modified significantly. In a companion work,<sup>38</sup> we are studying non-magnetic impurities in the triangular lattice antiferromagnet and explore spin liquid with a spinon Fermi surface, which may be relevant for the organic spin liquid material  $\kappa\text{-(ET)}_2\text{Cu}_2(\text{CN})_3$ .

#### Acknowledgments

We thank J. Alicea, M. P. A. Fisher, S. Ryu, and R. R. P. Singh for useful discussions and the A. P. Sloan Foundation for financial support (OIM).

<sup>1</sup> J. S. Helton, K. Matan, M. P. Shores, E. A. Nytko, B. M. Bartlett, Y. Yoshida, Y. Takano, A. Suslov, Y. Qiu, J.-H. Chung, D. G. Nocera, and Y. S. Lee, Phys. Rev. Lett. **98**, 107204 (2007).

<sup>2</sup> O. Ofer, A. Keren, E. A. Nytko, M. P. Shores, B. M. Bartlett, D. G. Nocera, C. Baines, and A. Amato, arXiv:cond-mat/0610540.

<sup>3</sup> T. Imai, E. A. Nytko, B.M. Bartlett, M.P. Shores, and D.

G. Nocera, arXiv:cond-mat/0703141.

<sup>4</sup> P. Mendels, F. Bert, M. A. de Vries, A. Olariu, A. Harrison, F. Duc, J. C. Trombe, J. S. Lord, A. Amato, and C. Baines, Phys. Rev. Lett. **98**, 077204 (2007).

<sup>5</sup> M. A. de Vries, K. V. Kamenev, W. A. Kockelmann, J. Sanchez-Benitez, and A. Harrison, arXiv:0705.0654.

<sup>6</sup> F. Bert, S. Nakamae, F. Ladieu, D. L'Hte, P. Bonville, F. Duc, J.-C. Trombe, and P. Mendels, arXiv:0710.0451.

- <sup>7</sup> A. Olariu, P. Mendels, F. Bert, F. Duc, J. C. Trombe, M. A. de Vries, and A. Harrison, arXiv:0711.2459.
- <sup>8</sup> S.-H. Lee, H. Kikuchi, Y. Qiu, B. Lake, Q. Huang, K. Habicht, and K. Kiefer, *Nature Materials* **6**, 853 (2007).
- <sup>9</sup> V. Elser, *Phys. Rev. Lett.* **62**, 2405 (1989); C. Zeng and V. Elser, *Phys. Rev. B* **42**, 8436 (1990).
- <sup>10</sup> J. T. Chalker and J. F. G. Eastmond, *Phys. Rev. B* **46** 14201 (1992).
- <sup>11</sup> P. W. Leung and V. Elser, *Phys. Rev. B* **47**, 5459 (1993).
- <sup>12</sup> P. Lecheminant, B. Bernu, C. L’huillier, L. Pierre, and P. Sindzingre, *Phys. Rev. B* **56**, 2521 (1997).
- <sup>13</sup> Ch. Waldtmann, H.-U. Everts, B. Bernu, C. Lhuillier, P. Sindzingre, P. Lecheminant, and L. Pierre, *Eur. Phys. J. B* **2**, 501 (1998).
- <sup>14</sup> P. Sindzingre, G. Misguich, C. Lhuillier, B. Bernu, L. Pierre, Ch. Waldtmann, and H.-U. Everts, *Phys. Rev. Lett.* **84**, 2953 (2000).
- <sup>15</sup> R. R. P. Singh and D. A. Huse, *Phys. Rev. Lett.* **68**, 1766 (1992).
- <sup>16</sup> N. Elstner and A. P. Young, *Phys. Rev. B* **50**, 6871 (1994).
- <sup>17</sup> G. Misguich and B. Bernu, *Phys. Rev. B* **71**, 014417 (2005).
- <sup>18</sup> M. Rigol and R. R. Singh, *Phys. Rev. Lett.* **98**, 207204 (2007); *Phys. Rev. B* **76**, 184403 (2007).
- <sup>19</sup> G. Misguich and P. Sindzingre, *Eur. Phys. J. B* **59**, 305 (2007).
- <sup>20</sup> S. Sachdev, *Phys. Rev. B* **45**, 12377 (1992).
- <sup>21</sup> F. Wang and A. Vishwanath, *Phys. Rev. B* **74**, 174423 (2006).
- <sup>22</sup> J. B. Marston and C. Zeng, *J. Appl. Phys.* **69**, 5962 (1991).
- <sup>23</sup> K. Yang, L. K. Warman, and S. M. Girvin, *Phys. Rev. Lett.* **70**, 2641 (1993).
- <sup>24</sup> M. B. Hastings, *Phys. Rev. B* **63**, 014413 (2001).
- <sup>25</sup> Y. Ran, M. Hermele, P. A. Lee, and X.-G. Wen, *Phys. Rev. Lett.* **98**, 117205 (2007).
- <sup>26</sup> Y. Ran, W.-H. Ko, P. A. Lee, X.-G. Wen, arXiv:0710.4574.
- <sup>27</sup> O. Ma and J. B. Marston, arXiv:0801.2138.
- <sup>28</sup> S. Ryu, O. I. Motrunich, J. Alicea, and M. P. A. Fisher, *Phys. Rev. B* **75**, 184406 (2007).
- <sup>29</sup> R. R. P. Singh and D. A. Huse, *Phys. Rev. B* **76**, 180407 (2007); arXiv:0801.2735.
- <sup>30</sup> H. Alloul, J. Bobroff, M. Gabay, P.J. Hirschfeld, arXiv:0711.0877.
- <sup>31</sup> A. Kolezhuk, S. Sachdev, R. R. Biswas, and P. Chen, *Phys. Rev. B* **74**, 165114 (2006).
- <sup>32</sup> B. Normand and F. Mila, *Phys. Rev. B* **65**, 104411 (2002).
- <sup>33</sup> S. Dommange, M. Mambrini, B. Normand, and F. Mila, *Phys. Rev. B* **68**, 224416 (2003).
- <sup>34</sup> G. B. Martins and W. Brenig, arXiv:0705.3985.
- <sup>35</sup> S. Eggert and I. Affleck, *Phys. Rev. Lett.* **75**, 934 (1995).
- <sup>36</sup> J. Oitmaa, C. Hamer, and W. Zheng, *Series Expansion Methods for Strongly Interacting Lattice Models*, (Cambridge University Press, Cambridge, 2006).
- <sup>37</sup> N. Elstner, R. R. Singh, and A. P. Young, *Phys. Rev. Lett.* **71**, 1629 (1993).
- <sup>38</sup> K. Gregor and O. I. Motrunich, “Knight shifts around non-magnetic impurities in a triangular lattice spin 1/2 anti-ferromagnet: Case of  $\kappa$ -(ET)<sub>2</sub>Cu<sub>2</sub>(CN)<sub>3</sub>”, in preparation.
- <sup>39</sup> In a one-dimensional (1d) chain with defects or with open boundaries, we studied the magnetization distribution in a projected Fermi sea state with small non-zero  $S_{\text{tot}}^z$ . In the mean field,  $m(x)$  oscillates along the chain as  $1+(-1)^x$  with a constant amplitude. We find that after the projection the staggered piece in fact grows away from the impurity as  $\sqrt{x}(-1)^x$ . This is consistent with the Eggert and Affleck prediction for the local susceptibility in the  $T = 0$  limit,<sup>35</sup> which is responsible for very strong NMR line broadening observed in 1d spin chain materials with impurities. On the other hand, in all our studies in two dimensions, we only found a fixed numerical enhancement rather than change in the qualitative behavior after the projection.
- <sup>40</sup> The broadening of the histograms of  $m_{\text{loc}}$  by about a factor of two upon the projection can be understood in the spirit of “Gutzwiller renormalizations”. For example, if we take a partially polarized mean field state and perform the projection exactly at one site, the corresponding local magnetization is increased by a factor  $1/(\langle n_{\uparrow} \rangle + \langle n_{\downarrow} \rangle - \langle n_{\uparrow} \rangle \langle n_{\downarrow} \rangle)$ , where the expectation values are in the free fermion system. For weak polarization  $\langle n_{\uparrow} \rangle \approx \langle n_{\downarrow} \rangle \approx 1/2$ , this factor is roughly 2. This simple reasoning treats only one site and does not take into account additional inter-site correlations introduced by the projection. This seems to work fine in the two-dimensional spin liquids that we studied but fails in one dimension.<sup>39</sup>
- <sup>41</sup> T. C. Hsu, *Phys. Rev. B* **41**, 11379 (1990).
- <sup>42</sup> O. I. Motrunich and M. P. A. Fisher, *Phys. Rev. B* **75**, 235116 (2007).